ZIBELINE INTERNATIONAL™ PUBLISHING

Environment & Ecosystem Science (EES)

DOI: http://doi.org/10.26480/ees.01.2023.01.12

ISSN: 2521-0882 (Print)
ISSN: 2521-0483 (Online)
CODEN: EESND2

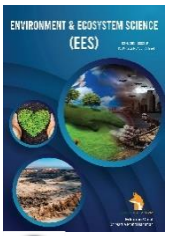

CrossMark

RESEARCH ARTICLE

THE IMPACT OF CLIMATE CHANGE ON SEDIMENT TRANSPORT CAPACITY: A CASE STUDY OF THE BOUBO COASTAL WATERSHED

Lenikpoho Karim Coulibaly [a,b*], **Naga Coulibaly** [c]

[a]*School of Geography and Information Engineering, China University of Geosciences, Wuhan, Hubei Province, China*
[b] *Zijin Mining Group Co., Ltd., 1 Zijin Rd, Shanghang, Fujian364200, China*
[c] *Department of Agriculture, Fishery Resources, and Agro-Industry, University of San Pedro, San Pedro, Côte d'Ivoire*
[*]*Corresponding Author E-mail: lenikpohokarim@gmail.com*

ARTICLE DETAILS

Article History:

Received 17 November 2022
Revised 20 December 2022
Accepted 24 January 2023
Available online 02 February 2023

ABSTRACT

For soil erosion modeling, determining sediment transport capacity (Tc) is essential because it plays a key role in sediment detachment, transport, and deposition research. This paper provides insights into the seasonal spatial distribution of sediment transport capacity, excess runoff depth in response to the distribution of precipitation, and land use at a watershed scale, using SCN Curve Number (CN) method, Remote Sensing (RS), and Geographic Information Systems (GIS). Spatial distribution in runoff production on hillslopes and sediment transport are explained. We integrated the effect of slope gradient in the curve number to model the landscape effect on sediment transport. The findings show that seasonal variation in sediment transport capacity is influenced by climate change. During June and October, the transport capacity is higher and coincides with channel areas in the Boubo watershed. Potential applications of this map may help the decision-maker to deal with problems associated with watershed development and management.

KEYWORDS

Sediment transport capacity, Soil Conservation Curve Number, GIS, Runoff

1. INTRODUCTION

Sediment transport capacity is described as the maximum amount of sediment carried by a given flow rate, and is explained in many erosion models (Xiao et al., 2017). Estimation of the transport capacity is essential for the process of sediment detachment, transport, and deposition, caused by rainfall and runoff impacts on the soil surface (Wang et al., 2019). Soil erosion associated with sediment production is a serious issue worldwide, which causes problems such as decreased soil fertility, degraded water quality, and reduced reservoir storage (Borrelli et al., 2017; Ciampalini et al., 2020; Garcia Ruiz et al., 2016; Lanckriet et al., 2016). Two main parameters associated with soil erosion are runoff and sediment yield (Zhu et al., 2018). Once runoff begins on the ground and in streams, the amount and size of material transported is determined by the runoff water's transport capacity (Tc). The excess sediment is deposited if the transport capacity is less than the amount of eroded soil available (Jain and Das, 2009; Jain et al., 2009). Sediment transport capacity must be considered when developing models of soil erosion in a GIS model that computes the spatial variability in erosion and deposition over the landscape (Wang et al., 2015). Therefore, it is crucial to study sediment transport capacity to help decision makers to deal with problems associated with watershed development, protection and management.

In recent decades, because of the use of remote sensing, GIS, and computing capacity, the investigations of runoff and sediment transport capacity models have been widely developed through spatially distributed models of watershed hydrological processes (Bolognesi et al., 2016; Hajigholizadeh et al., 2018; Roo, 1998; Van Dijk et al., 2016). Remote sensing and GIS techniques allow the user to import into the models a lot of information like canopy, slope, aspect, contributing drainage area, soil texture of various soil type, land use (Hajigholizadeh et al., 2018). Previous studies demonstrate that remote sensing technology and GIS can significantly enhance the traditional sediment transport and rainfall-runoff research (Nagarajan and Poongothai, 2012; Srinivas G et al., 2020; Van Rompaey et al., 2001; Verma et al., 2017).

In physically-based erosion models, sediment transport capacity is an important concept for determining detachment rates and deposition (Al-Hamdan et al., 2012; Hairsine and Rose, 1992). However, the link between soil detachment quantity and sediment load has been described from different points of view proposed a method for calculating soil detachment as a function of transport capacity, which was widely used, verified, and adopted by the water erosion prediction project (WEPP) model (Zhang et al., 2009; Foster and Meyer, 1972; Laflen et al., 1991). There are two main approaches for simulating sediment transport mechanisms: supply-limited and capacity-limited (Her, 2011). There are various types and equations for transport capacity relations in physically-based sediments transport models such as; Chemicals Runoff and Erosion from Agricultural Management Systems (CREAMS), WEPP, Kinematic Runoff and Erosion Model (KINEROS), Areal Nonpoint Source Watershed Environment Response Simulation (ANSWERS), Agricultural Non-Point Source Pollution (AGNPS), European Soil Erosion Model (EUROSEM), Revised Universal Soil Loss Equation 2 (RUSLE2), and LImburg Soil Erosion Model (LISEM) (Her, 2011; Kalin, 2003; Wang et al., 2019).

Recent studies used machine learning for the estimation of the sediment transport (Alizadeh et al., 2017; Chen and Chau, 2019; Reisenbüchler et al., 2021; Sharafati et al., 2020). However, machine learning technics use many and multiple data of training samples to develop a general and appropriate method. Research indicated that machine learning approach did not give good results because of the lack of data (Li et al., 2016). A group researcher describe the relationship between transport capacity, flow rate, and slope Gradient (Xiao et al., 2017). USDA-ARS pointed out that RUSLE2, a hybrid empirical/process-based model, can predict the

Quick Response Code	Access this article online	
	Website: www.environecosystem.com	**DOI:** 10.26480/ees.01.2023.01.12

Cite the Article: Lenikpoho Karim Coulibaly, Naga Coulibaly (2023). The Impact of Climate Change on Sediment Transport Capacity: A Case Study of The Boubo Coastal Watershed. *Environment & Ecosystem Science, 7(1): 01-12*.

transport capacity using runoff curve numbers (USDA-ARS, 2013). Also, studies have demonstrated that changes in Land Use/Land Cover (LULC) affect sediment yield in drainage channels worldwide (Alatorre et al., 2012). Therefore, it would be suitable to estimate runoff by integrating the curve number and LULC for the estimation of sediment transport in an area where data is limited.

The most important source of water for rivers, lakes, and ocean replenishment is rainfall to runoff flow, but water-runoffs cause significant hazards and disasters (Karamage et al., 2018). Infiltration and runoff data are essential inputs in estimating RUSLE2 rill sediment transport capacity developed by the hydrology Soil Conservation Service (SCS) (USDA-ARS, 2013). However, the rainfall-runoff generation procedure is extremely complex (Cristiano et al., 2017; David E. Fantina, 2012; Srinivasulu and Jain, 2009). There are different methods for estimating runoff, including spatial, empirical, and physical models (Devia et al., 2015; Sitterson et al., 2017). Some of the methods like the green roofs 2 model (GR2 model), the Green roofs 3 model (GR3 model), the rational Method, Synthetic unit Hydrograph Method have been used to estimate runoff (Seydou et al., 2018; Servat and Dezetter, 1993; Young et al., 2009; Patel and Thorvat, 2016). Estimating the amount of rainfall that exceeds infiltration and initial abstractions, which must be satisfied before the occurrence of runoff, is known as runoff rate estimation (Srinivas et al., 2020).

Rainfall depth is the major determinant of excess rainfall rate (USDA-ARS, 2013). The RUSLE2 assumption is that excess rainfall rate equals runoff depth divided by one hour. The resulting runoff values are indices of how runoff varies according to location as a consequence of climate change, cover management, and soil. Rainfall, runoff, and infiltration measurements were taken using various approaches based on the soil type, and hydrologic soil groups were created (Chow et al., 1988; Ross et al., 2018). For ungauged watersheds, accurate prediction of runoff from the ground into streams and rivers requires much effort and time, and Conventional methods of runoff measurements are not easy for inaccessible terrain, expensive, and time consuming (Gajbhiye, 2015). However, this information is critical in dealing with watershed planning, development, and management problems, as well as irrigation scheduling (Al-Ghobari et al., 2020; Gao et al., 2012).

Therefore, with the help of remote sensing and GIS, the curve number method could be used to calculate the possible runoff value in ungauged watersheds (Abdelaziz et al., 2020; Elhakeem and Papanicolaou, 2009; Gayathri and S, 2018; Köylü and Geymen, 2016; Nagarajan and Poongothai, 2012; Rietz and Hawkins, 2001; Strapazan and PetruȚ, 2017). Some researchers used NDVI, and other researchers used linear spectral mixture to estimate curve number (Fan et al., 2013; Gandini and Usunoff, 2004). The relationship between runoff and CN has already been established (Gebresellassie, 2017; Kim and Shin, 2018; Zhan and Huang, 2004). Generally, the CN is considered as a reliable and realistic method on location where available data on rainfall is limited but some studies indicated that the standard curve number method developed by SCS is not so effective in predicting overland flows in a semi-arid regions of Ethiopia ((Faizalhakim, 2018; Hong and Adler, 2008; Kinnell, 2010; Gebresellassie Zelelew, 2017).

The runoff CN approach is commonly used in hydrology because of Its simplicity, predictability, and stability (Gonzalez et al., 2015; Grimaldi et al., 2013; Ponce and Hawkins, 1996). It has been used for many years as it was adopted as an alternative to rational and other methods (Gao et al., 2012; Kim and Shin, 2019; Mishra and V.P., 2003). For natural disaster assessment, the SCS CN method is an effective and widely used approach for calculating the direct runoff from a storm event (Abdelaziz et al., 2020; Akhssas et al., 2020; Hong and Adler, 2008; Khaddor et al., 2015; NRCS, 1986). Water management and sediment transport may be carried out efficiently by knowing seasonal and annual runoff from the watershed. Also, the influence of slope on the curve number can be estimated using remote sensing and GIS (Huang et al., 2006; Meshram et al., 2015). Various watershed models, such as the Soil and Water Assessment Tools (SWAT), Storm Water Management Model (SWMM), and RUSLE2 use the curve number to determine runoff depth (Neitsch et al., 2011; Rossman, 2010; USDA-ARS, 2013). According to some research, the world is currently dominated by medium to high runoff potential, with curve numbers varying from 75 to 85 (Jaafar et al., 2019).

The methodology used in this study is based on integrating slope in the estimation of the curve number map used to estimate runoff in the Boubo coastal watershed. We used linear regression to produce a monthly sediment transport capacity map. This study aims to estimate the spatial distribution of the sediment transport capacity, using SCS CN to determine the runoff in an ungauged watershed. The objectives were first to estimate the CN, second to estimate runoff in the watershed, and finally to estimate the sediment transport capacity. The proposed framework is applied to the Boubo watershed to estimate its RUSLE2 rill transport capacity. The Boubo coastal watershed is critical for the physical, biological, and hydrological exchange between lagoons and the sea. However, monitoring projects fail to take into account their rivers (Coulibaly et al., 2021; Sébastien et al., 2013). Furthermore, this important large coastal watershed presents a lack of hydrologic and hydrometric stations, which cannot reflect the climate variation, which makes studies difficult in this watershed. Boubo coastal watershed ecosystems and fishing resources are highly threatened. This framework is used to analyze and estimate the spatial variation of sediment transport in the Boubo watershed, which can provide useful information to help decision-makers to formulate policies to protect the ecosystem degradation of the study region.

2. Study Area

The study area is the Boubo watershed, which is located in Côte d'Ivoire (Figure 1). The total watershed area is 5048.27 km2 (Table 1). The climate is the Sub-equatorial type (two rainfall seasons), with a rainfall of over 1500 mm/year. The average temperature in the basin oscillates between 25 ° C and 27 ° C. We used Digital Elevation Model (DEM) from Alos Palsar (https://www.asf.alaska.edu) to extract the watershed boundary, and elevation data in digital form, which is required for generating the flow delineation, the flow direction, and the flow networks in a given watershed.

Table 1: Geographical and Hydrologic Features of the Boubo Watershed

Boubo coastal watershed	Area (km2)	Mean Slope(%)	Length (km)	Mean CN
	5048.27	8.47	578.08	80.83

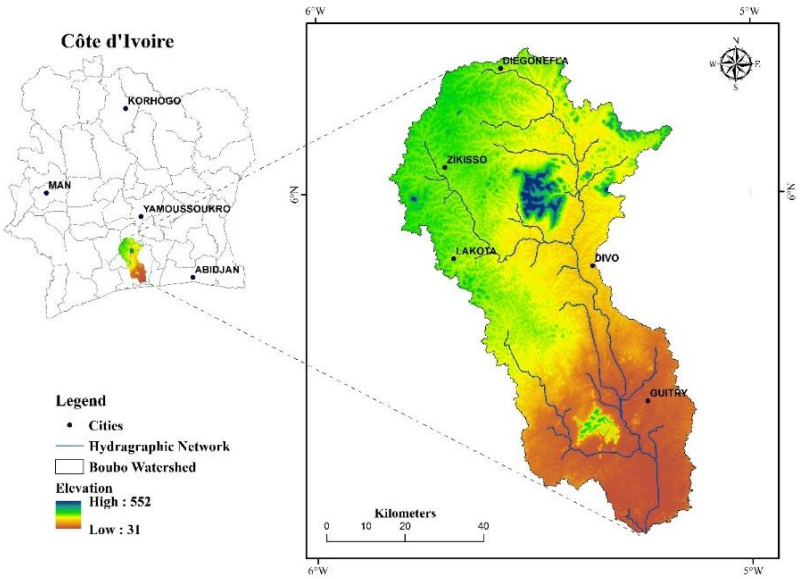

Figure 1: Boubo Watershed

3. METHOD

We developed a distributed model by grid cell to spatially represent sediment transport in each month of the year 2020 in the Boubo coastal watershed.

3.1 Estimation of Sediment Transport Capacity

Figure 2 exhibits the methodology used in this study to estimate the sediment transport capacity.

The sediment transport capacity of runoff in rill areas is calculated using the RUSLE2 equation (USDA-ARS, 2013):

$$T_c = K_T qs \quad (1)$$

where: the coefficient K_T coefficient for sediment transportability computed as a function of the cover management variable, q represents the runoff, and s denotes the sin of the slope angle. The product qs represent the runoff erosivity. The RUSLE2 calibrated value for K_T is K_T= 4004.62t/m³ (USDA-ARS, 2013).

3.1.1 Estimation of Runoff

RUSLE2 uses the NRCS-CN method to compute runoff depth as a function of precipitation amount and curve number (Haan et al., 1994; Ibrahim et al., 2022). Curve number values vary with cover-management, hydrologic soil group, and antecedent soil moisture (Ibrahim et al., 2022; NRCS, 1986). We used RS and GIS data to map probable runoff depth in different land use, soil texture, and slope. The NRCS curve number equation computes runoff depth as:

$$Q = \frac{(P - 0.2S)^2}{P + 0.8S}, if\ P > 0{,}2S \quad (2)$$

$$Q = 0\ , if\ P \leq 0{,}2S \quad (3)$$

where: Q = runoff depth or excess rainfall (mm), P = precipitation depth (mm), and S = a variable of potential retention capacity (mm) computed with:

$$S = \left(\frac{25400}{CN}\right) - 254\ \ in\ mm, SI\ units \quad (4)$$

Where: CN= the runoff curve number (dimensionless) 0 ≤ CN ≤ 100, and S represents the potential maximum soil retention (S). Some researchers used this methodology to estimate the runoff depth for all the specific days of the year (Boughton, 1989; Mishra S.k. and V.P., 2003; USDA, 2004a). This study was carried out using the long-term mean monthly runoff.

3.1.2 Estimation of Rainfall

Precipitation is an important input variable in hydrological models, and its spatial variation affects the hydrological response predicted by distributed models (Fu et al., 2011; Komuscu and Legate, 1999). The assumption of spatial invariance of the effective rainfall is hardly applicable to catchment areas greater than 5000 km². The non-uniform distribution of rainfall can cause variation in the hydrograph shape (Mishra S.k. and V.P., 2003; Sachan et al., 2015). Rainfall, the chief source of surface runoff, was used as input to estimate runoff depth. The monthly distribution of maximum rainfall data of the Boubo watershed for the past 30 years from 1990 to 2020 was obtained from the NASA POWER website (https://power.larc.nasa.gov). The data have been analyzed, and the kriging method was used to represent the spatial distribution of rainfall.

3.1.3 Estimation of the Curve Number

3.2 Preparation of Hydrological Soil Group (HSG) Map

Soil parameters influence the process of generation of runoff from rainfall, and they must be considered in the methods of runoff estimation (Srinivas G et al., 2020). Soil properties that affect runoff are clay in the top layer, average clay content in the profile, infiltration, and permanent soil texture (Rawat and Singh, 2017). Soils data and the sand, silt, and clay fractions as well as the percentage of organic matter come *f*rom the Digital Soil Map of the world (DSMW) produced by the Food and Agriculture Organization of the United Nations (http://www.fao.org) (Figure 3). Soil infiltration rates differ widely and are influenced by subsurface permeability. Four hydrologic classes exist in soil classification, HSG" s (A, B, C, and D), based on their minimum infiltration rate, determined after prolonged wetting for the bare soil. Previous studies describe the HSG according to soil texture (NRCS, 2009). The study area includes sandy clay loam, sandy clay, and clay soil textures (Coulibaly et al., 2021). The hydrological soil group map in the Boubo watershed (Figure 4), which refers to the soil's infiltration capacity, was extracted and classified from the global gridded hydrologic soil groups for curve number-based runoff modeling (Ross et al., 2018). Ross et al. (2018) created a globally consistent gridded dataset that defines appropriate HSGs for regional to global scale modeling.

3.2.1 Hydrological Characteristics of The Soil Moisture Conditions Which Are Expressed by The Antecedent Moisture Condition (AMC)

In theory, the longer the slope, the more runoff will occur. However, the impact of slope length on runoff is not clear yet, sometimes positive, sometimes nil, and sometimes negative, according to the antecedent moisture and condition of the soil surface (Roose, 1996). Therefore, it is essential to estimate the antecedent soil moisture condition. NRCS has identified three types of multi-level humidity conditions (antecedent moisture condition) as land-based factor that affects CN, precisely: dry (condition 1, the wilting point has not been reached), the mean (condition 2), and saturated water (condition 3). Curve numbers corresponding to AMC-I and AMC-III conditions can be computed from AMC -II. The CN shown in Table 3 corresponds to AMC II. Sobhani (1976) developed the following algebraic expressions for calculating CNI and CNIII from CNII (Boughton, 1989)

$$CN_I = \frac{CN_{II}}{2.334 - 0.01334 CN_{II}} \quad (5)$$

$$CN_{III} = \frac{CN_{II}}{0.427 + 0.00573\ CN_{II}} \quad (6)$$

As for the soil moisture conditions, curve numbers are based on the Antecedent Moisture Condition (AMC) index (Table 2), which refers to the antecedent moisture content in the soil five days before the beginning of the rainfall-runoff event that is being studied (Chow V.T. et al., 1988; Matomela et al., 2019; Vojtek and Vojteková, 2016). The average condition (AMC-II) is used in this analysis to determine the CN value for the study region because a moderate antecedent soil moisture condition is used in RUSLE2 (USDA-ARS, 2013).

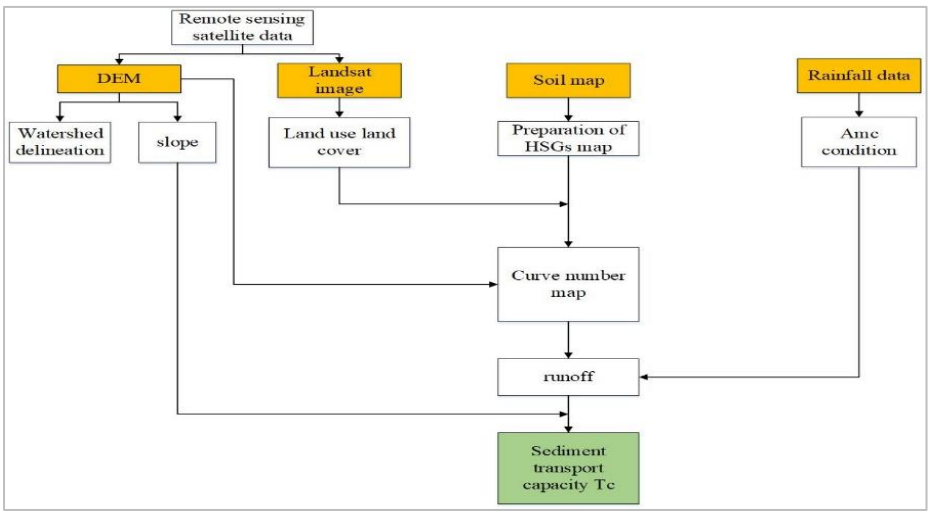

Figure 2: Flowchart showing the methodology employed by the GIS-based CN model in estimating the sediment transport capacity

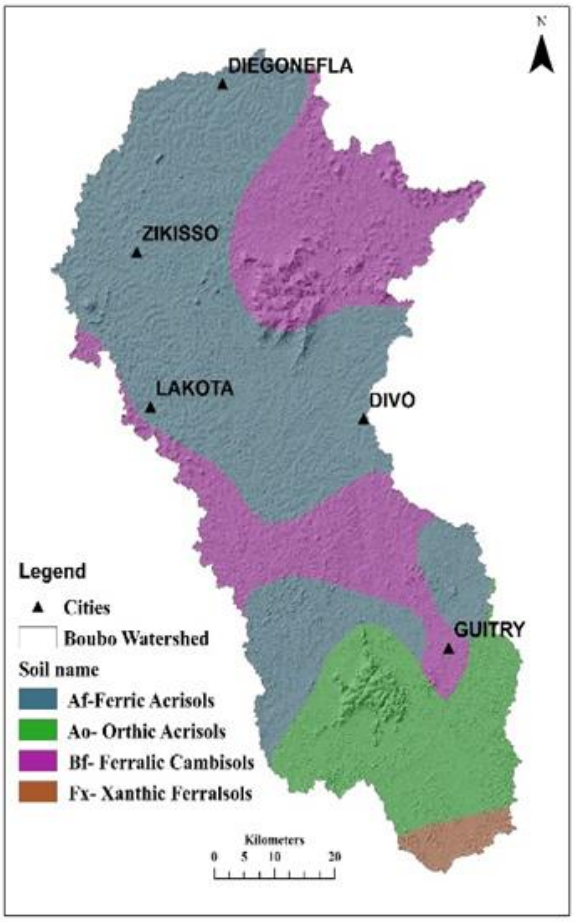

Figure 3: Soil types in the Boubo Watershed

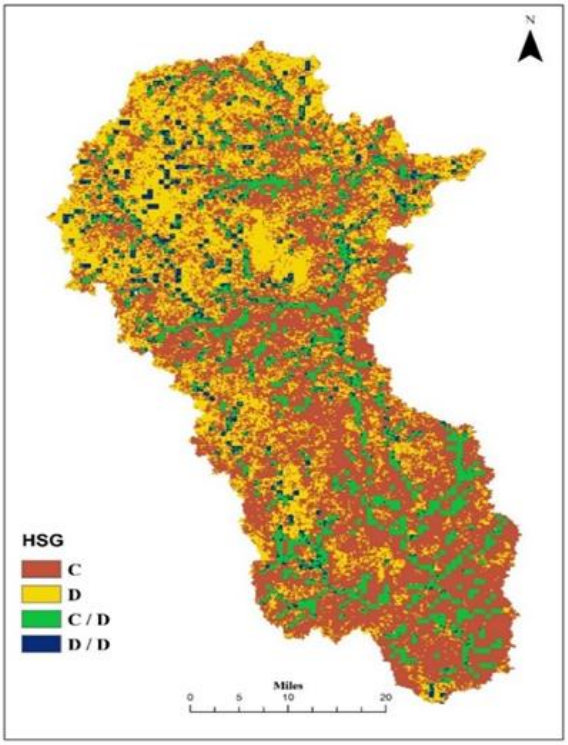

Figure 4: Hydrologic soil group of the Boubo watershed

Table 2: Classification of the Antecedent Soil Moisture Condition (AMC) and the Related Curve Number (CN) Source: Soil Conservation Service, 1972)

AMC Group	Curve Number CN	Description	Total 5-Days Antecedent rainfall (mm)	
			Dormant Season	Growing Season
I	CN_I	Lowest runoff potential	Less than 12,7	Less than 35,6
II	CN_{II}	Average condition	12,7 to 27,9	35,6 to 53,3
III	CN_{III}	Highest runoff potential	Over than 27,9	Over than 53,3

3.2.1.1 Slope-Adjusted

The CN value must be estimated precisely to achieve accurate predictions of surface runoff (Kim and Lee, 2008). The slope is an essential factor determining water movement within the landscape and may affect runoff (Ajmal et al., 2020; Chaplot and Le Bissonnais, 2003). We used the slope-adjusted CN approach to improve and integrate the slope into the runoff analysis. The $CN_{II\alpha}$ is then used, instead of CN_{II}, in the calculations of the runoff depth. The slope-adjusted $CN_{II\alpha}$ equation is (Huang et al., 2006):

$$CN_{II\alpha} = \left(\frac{CN_{III} - CN_{II}}{3}\right)(1 - 2e^{-13.86\alpha}) + CN_{II} \quad (7)$$

Where: $CN_{II\alpha}$ is slope-adjusted CN for normal conditions; CN_{II} and CN_{III} are tabulated curve numbers dependent on basin characteristics for normal and wet conditions, respectively; and α is the average soil slope of the watershed (m/m).

3.2.1.2 Weighted Curve Number

The slope-adjusted curve numbers were computed using the weighted average concerning the contributing area of the discharge profile in different land use. For the estimation of the CN_I and CN_{III} based on equations (5) and (6), we need to first estimate CN_{II}. In this study, CN_{II} has been adjusted for the Boubo watershed by weighting curve numbers with respect to watershed/land cover area, to obtain CN_{aw}. The CN_{aw} is then used to derive CN_{III} using equation (6). Finally, we obtained $CN_{II\alpha}$ by using CN_{III} and CN_{aw} in equation (7). The weighted area curve number CN_{aw} used to estimate $CN_{II\alpha}$ of the group of soil and surface of land cover type is:

$$CN_{aw} = \frac{\sum_{i=1}^{n} CN_i * A_i}{A} \quad (8)$$

Where: CN_{aw} = weighted curve number. CN_i = curve number from one to any n area A_i with curve number CN_i; A = overall area of the watershed.

3.2.2 Preparation of Soil Cover Complex Cngrid Preparation From Landuse and Soil Type

Soil cover complex map is prepared by integrating hydrological soil group map and land use map. Previous studies provide tables and graphs of runoff curve numbers (Chow V.T. et al., 1988; Mishra S.k. and V.P., 2003; USDA, 2004b; Victor Mockus, 2017). It was necessary to know the hydrological characteristics of the land use categories in the watershed with their respective curve numbers to obtain Table 3. CN values were determined by mapping land cover classes of the Global Land Cover (GLC) with Fine Classification System at 30m in 2020 (Figure 5). The GLC land cover classes are classified into various plant functional types, and a detailed description for each land cover class is provided by (Liangyun, 2020).

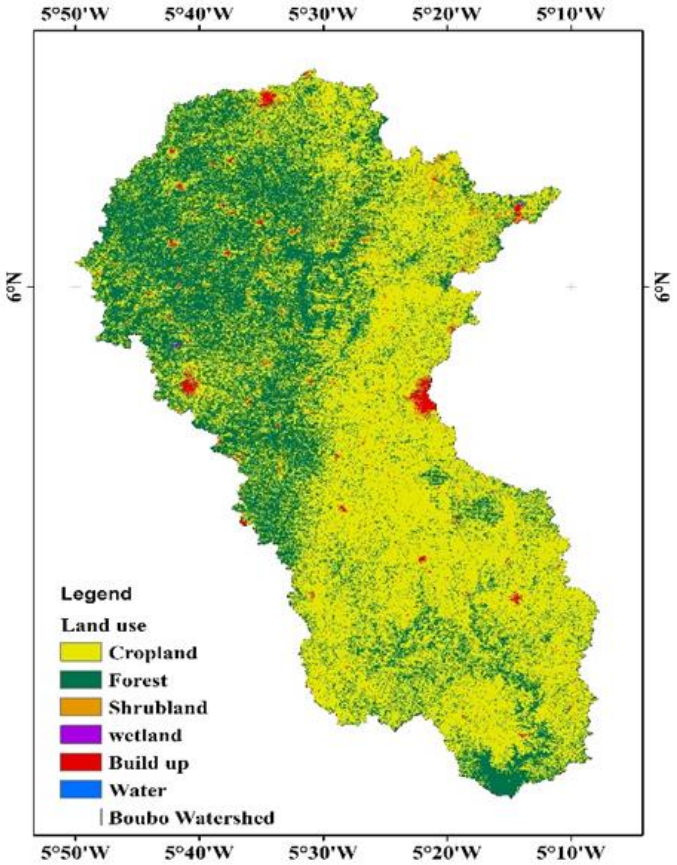

Figure 5: Land Use Land Cover classification

Table 3: Curve Number Values for Land Use Categories in the Boubo Watershed.

No	LUValue	Land use	Hydrologic condition	Runoff curve numbers for hydrological soil groups			
				A	B	C	D
1	1	Cultivated land	Good	67	78	85	89
2	2	Forest	Good	30	55	70	77
3	3	Shrubland	Shrub (good), and Brush (fair)	42	62	75	81
4	4	Wetland	-	100	100	100	100
5	5	Built up	65% impervious and the remaining pervious areas are considered to be in good pasture condition	77	85	90	92
6	6	Water	-	100	100	100	100

4. RESULTS

The sediment transport capacity was spatially modeled within the Boubo watershed by applying the described methods. The SCS-CN model is used to calculate runoff depth from daily rainfall depths. The runoff was computed and predicted using LULC, hydrological soil cover, and antecedent moisture condition variables. The CN values were estimated for different land use of the watersheds, and the slope-adjusted $CN_{II\alpha}$ for different cells were calculated to better represent the CN in the study area. This study suggests the use of GIS to provide a variety of maps, including maps of land use and watershed curve number map (Figure). The monthly sediment transport capacity map (Figure 10), is suitable and can quickly and accurately guide the user information.

4.1 Rainfall Map

The spatial distribution of rainfall value was found to vary from 21.21 in January to 341.59 in June in the Boubo watershed (Figure 6). The maximum rainfall is located in the southern part of the watershed around the coastal area. The study area presents a high climate variability in the year 2020 due to seasonal climate change.

4.2 SCS-CN Runoff Model

4.2.1 Slope-Adjusted

In the GIS-based SCS-CN model, the CN is used as input to compute runoff depth. For different curve numbers, the runoff was calculated for AMC II conditions. The runoff depth values were computed using equation (2). CN_{III} values associated with AMC-III were determined using equation (6) to derive slope-adjusted ($CN_{II\alpha}$). Figure shows that the $CN_{II\alpha}$ slope adjusted values range from 70 in forest areas to 100 in wetland areas and water bodies. The highest slope-adjusted $CN_{II\alpha}$ (92 and 100) was associated with a steep slope, built-up areas, and water bodies, while the medium slope-adjusted $CN_{II\alpha}$ (78.40) was found in the forest areas associated with slopes <20%. The lower the number, the lower the runoff potential, and the higher the number, the higher the runoff potential. Table shows the curve numbers obtained from the HSG and five LULC classes.

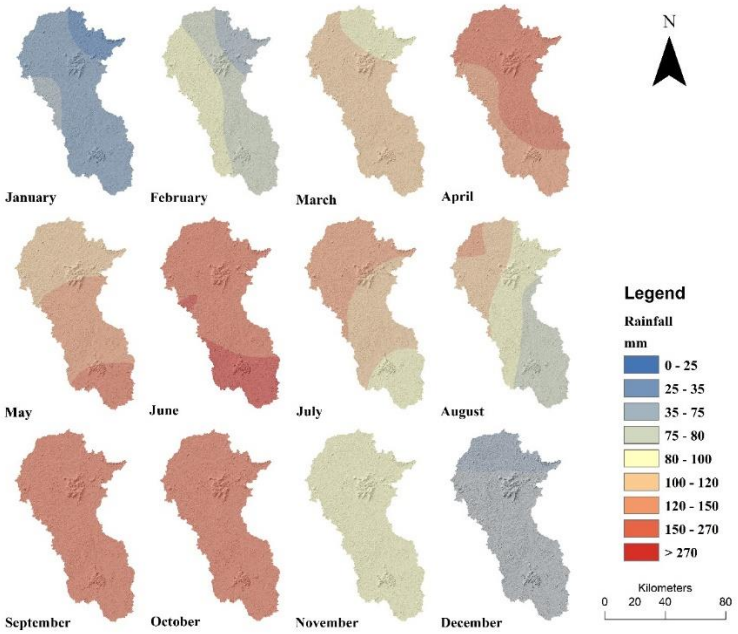

Figure 6: Rainfall distribution map of the study area.

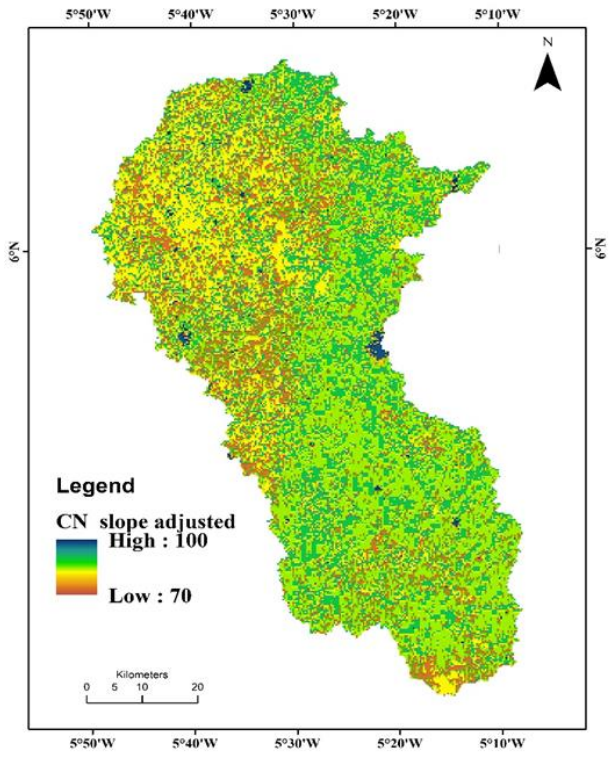

Figure 7: Curve number slope adjusted map

Table 4: Weighted Curve Number Based on Soil, HSG, nd the Surface of Land Cover Type						
No	Land cover	HSG	CN	Year 2020		
				Area (km2)	Area (%)	CN* Area (%)
1	Cultivated land	C	85	2135.250	42.297	3595.217
		D	89	876.091	17.354	1544.531
2	Forest	C	70	1035.350	20.509	1435.630
		D	77	878.044	17.393	1339.259
3	Shrubland	C	75	57.169	1.132	84.933
		D	81	22.060	0.437	35.396
4	wetland	C	100	0.747	0.015	1.480
		D	100	0.484	0.010	0.958
5	Built up	C	90	30.409	0.602	54.212
		D	92	12.235	0.242	22.298
6	Water	C	100	0.095	0.002	0.188
		D	100	0.339	0.007	0.672
	TOTAL			5048.27	100	8114.775

4.2.2 Potential Maximum Retention Map

The potential maximum retention (S) is calculated using equation (4), and the spatial distribution is shown in Figure 8. The values of S range from 0 to 108.857 mm. The lowest S values within the watershed are located in built-up areas, where the retention capacity is low. Cropland and forest areas have the highest S values as they have a high retention capacity. The mean potential maximum retention was 56.05 mm in the year 2020.

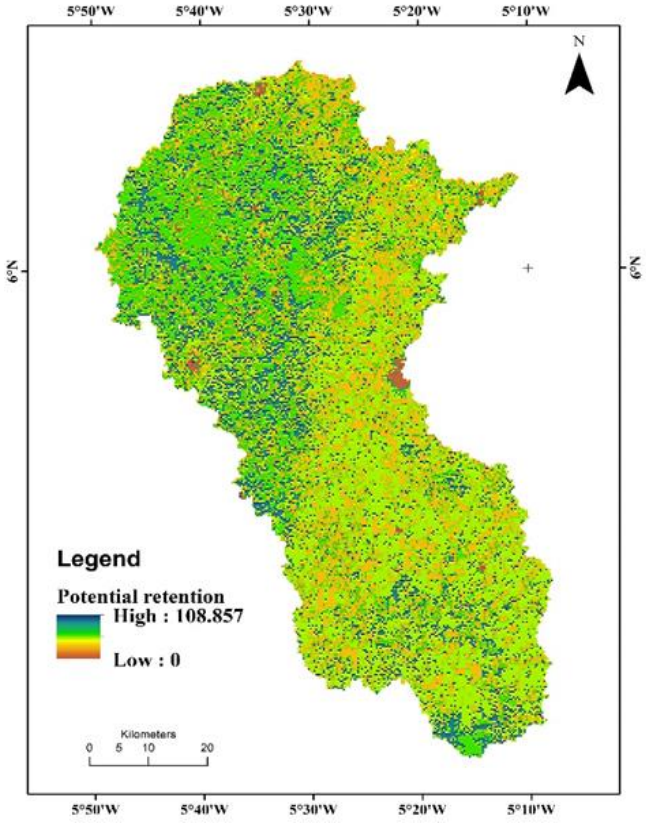

Figure 8: Potential maximum retention (S) map of the Boubo coastal watershed

4.2.3 The Soil Conservation Service Runoff Depth

The spatial processes in runoff models provide a mean in representing the watershed. The changes in vegetation and precipitation impact runoff. Runoff depth is shown in Figure , where the values range from 0.046 mm to 320.3 mm depending on the retention capacity of individual surfaces during a month. The Soil Conservation Service Runoff depth was calculated using equations (2) and (3). The lowest values of runoff depth occur in January and December in the Boubo, which is caused on one hand by the high potential of water interception by the forest and, on the other hand, by water retention due to predominantly sandy clay loam and clay of soil texture. Built-up areas are the most vulnerable to surface runoff, with CN numbers often exceeding 85. The Boubo coastal watershed also contains areas vulnerable to erosion and mostly correspond with the areas of high depth of surface runoff. Simulations of runoff in a distributed spatial process can help to understand how changes in the environment affect runoff and the hydrological cycle.

4.2.4 Sediment Transport Capacity

The amount of eroded soil particles moving from upstream cells to downstream cells and finally to the watershed outlet depends on the transporting capacity of the flowing water. A monthly value of spatially distributed sediment transport capacity for all cell areas was computed using equation (1). Rainfall change affects the average monthly transport capacity, which varies from month to month. As shown in Figure, the areas showing higher transport capacity coincide with channel areas in the watershed. Smaller transport capacity values are mainly found to be associated with the forest regions and flatter land areas found in the cultivated lands in the watershed. The seasonal variation of the rainfall also affects the sediment transport capacity.

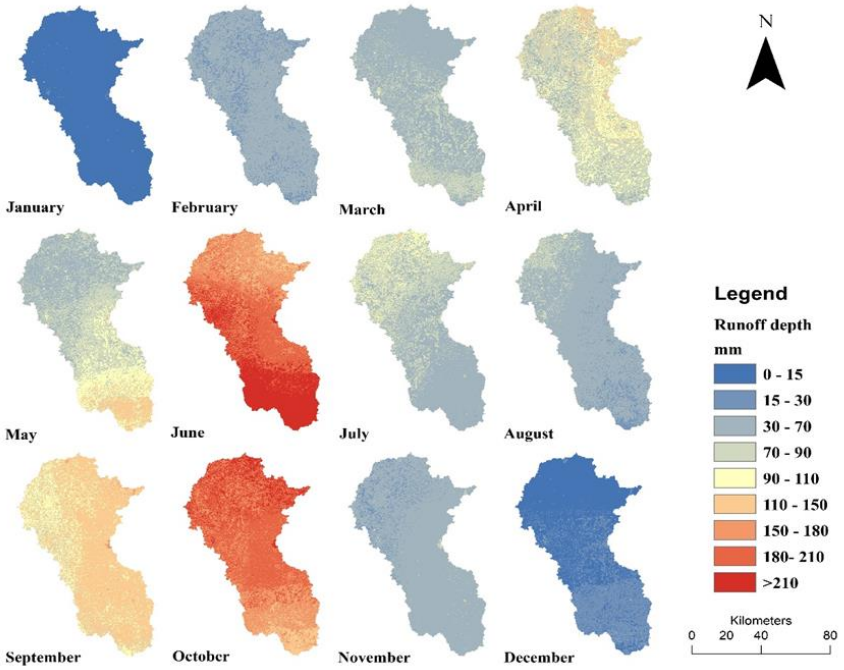

Figure 9: SCS-Runoff depth map

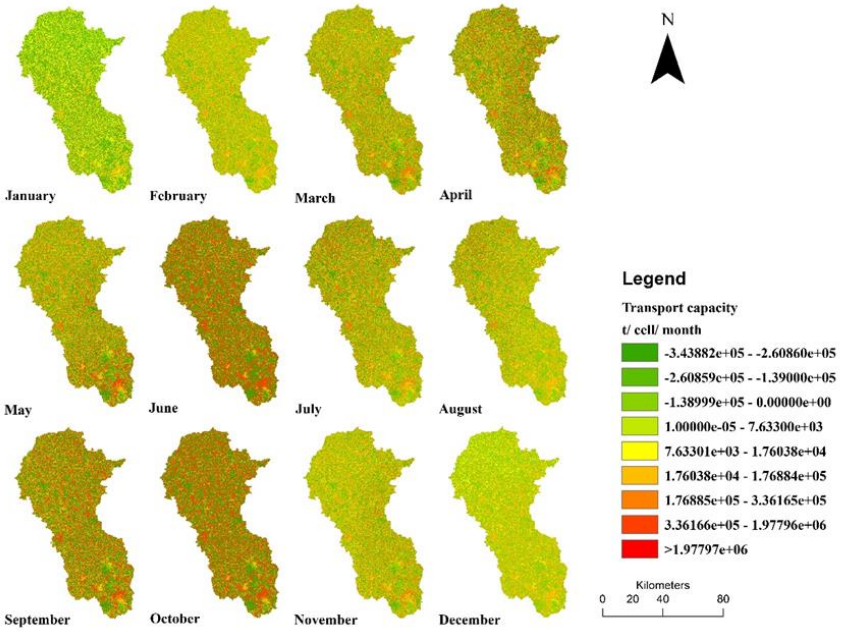

Figure 10: Map of the RUSLE2 sediment transport capacity during the year 2020

5. Discussion

The main goal of this study was to estimate the seasonal spatial distribution of the sediment transport capacity, using SCS CN to determine the runoff in an ungauged watershed. Climate, measured runoff, and soil data are important in sediment transport modeling. The estimation of runoff depends on climate and soil data. However, monitoring measurements of runoff and sedimentation in the Boubo coastal watershed did not exist. In Côte d'Ivoire, it is difficult to conduct accurate studies in some areas because of the lack of field-measured data. Similarly, in Africa, the paucity of collecting data was also noticed (Borrelli et al., 2021; Lal, 2009; Vanmaercke et al., 2014). Therefore, in the Boubo watershed, remote sensing and GIS are excellent options to map the monthly spatial distribution of the sediment transport capacity in an ungauged watershed. A long-term data record is needed in the watershed to conduct future research.

The HSG C and D dominate the watershed and have a high drainage potential. Divo, Lakota, Guitry, and Diegonefla were found to have high runoff potential dominated by the hydrological soil group C. Indeed, the association of HSG and LULC could help to know the infiltration capacity of the soil. In Divo city, the ability of runoff to infiltrate into the surface is limited by human-made structures (roads, buildings). This study reveals that rainfall variation impact significantly runoff and the sediment transport. Similarly, Abdelaziz et al. (2020) indicated that precipitation change has a great influence on runoff and water quality in Abidjan city. Comparing the behavior of runoff and sediment transport capacity in natural areas such as forests to man-made construction like cities give us an idea of how easily human activities and seasonal rainfall change can impact sediment transport.

June and October were found to have a higher rate of sediment transport. This high rate was linked to a high rainfall rate during June and October. The seasonal spatial distribution of the sediment transport capacity indicated how climate change affects sediment movements. Although curve number approach gives satisfactory results in ungauged watershed, it must be noted that curve number method use cover management, soils, and runoff to estimate the sediment transport. Many models exist, in particular Support Vector Machine (SVM), Artificial neural network (ANN) which can be a suitable alternative (Reisenbüchler et al., 2021; Sharafati et al., 2020). However, the soft computing method needs many data to train the model and develop a standard and replicable method. More data

collection is needed in the coastal area to evaluate the suitable method. Evaluation of the suspended sediment and bedload sediment is important in the selection of a suitable method in this area. Further study could evaluate how soft computing techniques perform in estimating the sediment transport capacity compared to the RUSLE2 sediment transport capacity concept presented here.

There are many ways conservation planning can address these environmental issues. Planting trees can help because some plants have natural ways of preventing erosion from occurring and limiting the amount of damaging runoff into waterways. These issues can be addressed by increasing public awareness and sparking discussions about how these can harm the environment. The active implementation of soil and water conservation and sediment control programs is needed in the Boubo watershed and can reduce sediment loads or reduce the problem associated with removing surfaces. Similarly, researchers indicated that improved sediment monitoring programs in many areas of the world, particularly in developing countries, are needed (Walling, 2009).

6. Limits of This Study

The accuracy of the results strongly depends on the accuracy of the data used. The methodology used for sediment transport capacity and runoff estimation presents some advantages and limitations. First, the rainfall spatial and temporal distribution will influence the initial abstraction and CN values. At the same time, the SCS-CN model does not consider them. Therefore, the effects caused by these factors on estimation accuracy and model efficiency are inevitable in its extensive promotion and long-term application. Second, direct runoff volume is assumed to equal excess rainfall volume when the CN method is applied at a field scale or grid-based distributed modeling. If it were used to calculate only excess rainfall contributing to direct runoff generated on an isolated field or cell, the assumption would be valid because rainfall is the only source of direct runoff there. However, a cell might have two sources of direct runoff, rainfall and routed runoff volume from upstream areas when distributed overland routing is utilized in distributed modeling. Thus, the applicability of a traditional CN method should be limited when distributed overland routing is incorporated into a distributed modeling practice. Finally, the SCS-CN model is a lumped model used to simulate rainfall-runoff; i.e., there is an input value of rainfall and an output value of runoff. The model ignores the time variation of infiltration or the cumulative runoff processes during the calculation but considers space and temporal variation. However, in this study, we integrated the effect of slope gradient in the curve number to model landscape effect on sediment transport. Additionally, the division of soils into hydraulic groups is very coarse, and the definition of antecedent moisture condition is not quantitative. These disadvantages of the SCS-CN model exclude its application for some process-based purposes but guarantee the model's simplicity and stability in estimating runoff.

7. Conclusion

The present study investigated the seasonal spatial distribution of the RUSLE2 sediment transport capacity in an ungauged watershed. GIS data collection is cost-effective for various planning scenarios. The combination of GIS tools, remote sensing, and the NRCS curve number model is easier and faster in ungauged watersheds to generate runoff and sediment transport maps. Previous studies did not use a distributed model based the RUSLE2-GIS-based approach to estimate the sediment transport capacity in this area. The model provides engineers and planners with an efficient and useful tool for planning and conservation purposes. Results show that rainfall runoff significantly influences sediment transport capacity in Boubo and Tc is high especially in June and October. Human-made structures limit runoff's ability to infiltrate into the surface in Divo, Guitry, Lakota, and Diegonefla Cities.

However, the runoff results of this study are limited to the validity of the rainfall data of the Boubo watershed. For the replication of such a study, more physical and climatic settings are imperative for indicating its common applicability in sediment transport studies. More data measurement may further help refine the results of the present study. The appropriate soil and water conservation measures should be planned and implemented in the watershed to protect the ecological environment. The study area requires suitable water management programs to minimize water flow-related disasters and water pollution. Future studies should evaluate and compare the performance of the machine learning approach to RUSLE2 sediment transport capacity method in this area.

References

Abdelaziz, K.K., Nicaise, Y., Séguis, L., Ouattara, I., Moussa, O., Auguste, K., Kamagaté, B. and Diakaria, K., 2020. Influence of Land Use Land Cover Change on Groundwater Recharge in the Continental Terminal Area of Abidjan, Ivory Coast. Journal of Water Resource and Protection, 12 (05), Pp. 431-453. https://www.doi.org/10.4236/jwarp.2020.125026.

Ajmal, M., Waseem, M., Kim, D., and Kim, T.W., 2020. A Pragmatic Slope-Adjusted Curve Number Model to Reduce Uncertainty in Predicting Flood Runoff from Steep Watersheds. Water, 12 (5). https://www.doi.org/10.3390/w12051469.

Akhssas, A., Jabri, B., Hessane, M.A., Baba, K., Bahi, L., Benradi, F., Cherkaoui, E., Khamar, M., Lahmili, A., Menzhi, M., Nounah, A. and Ouadif, L., 2020. Production of a Curve Number map using GIS Techniques in the watershed of the high Sebou (Morocco). E3S Web of Conferences, 150. https://doi.org/10.1051/e3sconf/202015003003.

Alatorre, L.C., Beguería, S., Lana-Renault, N., Navas, A. and García-Ruiz, J.M., 2012. Soil erosion and sediment delivery in a mountain catchment under scenarios of land use change using a spatially distributed numerical model. Hydrology and Earth System Sciences, 16 (5), Pp. 1321-1334. https://doi.org/10.5194/hess-16-1321-2012.

Al-Ghobari, H., Dewidar, A. and Alataway, A., 2020. Estimation of Surface Water Runoff for a Semi-Arid Area Using RS and GIS-Based SCS-CN Method. Water, 12 (7). https://www.doi.org/10.3390/w12071924.

Al-Hamdan, O.Z., Pierson, F.B., Nearing, M.A., Stone, J.J., Williams, C.J., Moffet, C.A., Kormos, P.R., Boll, J. and Weltz, M.A., 2012. Characteristics of concentrated flow hydraulics for rangeland ecosystems: implications for hydrologic modeling. Earth Surface Processes and Landforms, 37 (2), Pp. 157-168. https://www.doi.org/10.1002/esp.2227.

Alizadeh, M.J., Jafari Nodoushan, E., Kalarestaghi, N., and Chau, K.W., 2017. Toward multi-day-ahead forecasting of suspended sediment concentration using ensemble models. Environ Sci Pollut Res Int, 24 (36), Pp. 28017-28025. https://www.doi.org/10.1007/s11356-017-0405-4.

Bolognesi, M., Farina, G., Alvisi, S., Franchini, M., Pellegrinelli, A. and Russo, P., 2016. Measurement of surface velocity in open channels using a lightweight remotely piloted aircraft system. Geomatics, Natural Hazards and Risk, 8 (1), Pp. 73-86. https://www.doi.org/10.1080/19475705.2016.1184717.

Borrelli, P., Alewell, C., Alvarez, P., Anache, J.A.A., Baartman, J., Ballabio, C., Bezak, N., Biddoccu, M., Cerda, A., Chalise, D., Chen, S., Chen, W., De Girolamo, A.M., Gessesse, G.D., Deumlich, D., Diodato, N., Efthimiou, N., Erpul, G., Fiener, P., Freppaz, M., Gentile, F., Gericke, A., Haregeweyn, N., Hu, B., Jeanneau, A., Kaffas, K., Kiani-Harchegani, M., Villuendas, I.L., Li, C., Lombardo, L., Lopez-Vicente, M., Lucas-Borja, M.E., Marker, M., Matthews, F., Miao, C., Mikos, M., Modugno, S., Moller, M., Naipal, V., Nearing, M., Owusu, S., Panday, D., Patault, E., Patriche, C.V., Poggio, L., Portes, R., Quijano, L., Rahdari, M.R., Renima, M., Ricci, G.F., Rodrigo-Comino, J., Saia, S., Samani, A.N., Schillaci, C., Syrris, V., Kim, H.S., Spinola, D.N., Oliveira, P.T., Teng, H., Thapa, R., Vantas, K., Vieira, D., Yang, J.E., Yin, S., Zema, D.A., Zhao, G. and Panagos, P., 2021. Soil erosion modelling: A global review and statistical analysis. Sci Total Environ, 780, Pp. 146494. https://www.doi.org/10.1016/j.scitotenv.2021.146494.

Borrelli, Robinson, D.A., Fleischer, L.R., Lugato, E., Ballabio, C., Alewell, C., Meusburger, K., Modugno, S., Schutt, B., Ferro, V., Bagarello, V., Oost, K.V., Montanarella, L. and Panagos, P., 2017. An assessment of the global impact of 21st century land use change on soil erosion. Nature communications, 8 (1), Pp. 2013. https://www.doi.org/10.1038/s41467-017-02142-7.

Boughton, W., 1989. A review of the USDA SCS curve number method. Australian Journal of Soil Research, 27 (3), Pp. 511. https://doi.org/10.1071/sr9890511

Chaplot, V.A.M., and Le Bissonnais, Y., 2003. Runoff Features for Interrill Erosion at Different Rainfall Intensities, Slope Lengths, and Gradients in an Agricultural Loessial Hillslope. Soil Science Society of America Journal, 67 (3), Pp. 844-851. https://www.doi.org/10.2136/sssaj2003.8440.

Chen, X.Y., and Chau, K.W., 2019. Uncertainty Analysis on Hybrid Double Feedforward Neural Network Model for Sediment Load Estimation with LUBE Method. Water Resources Management, 33 (10), Pp. 3563-3577. https://www.doi.org/10.1007/s11269-019-02318-4.

Chow, V.T., Maidment, D.R., and Mays L.W., 1988. Applied hydrology, New Delhi.

Ciampalini, R., Constantine, J.A., Walker-Springett, K.J., Hales, T.C., Ormerod, S.J. and Hall, I.R., 2020. Modelling soil erosion responses to climate change in three catchments of Great Britain. Sci Total Environ, 749, Pp. 141657. https://doi.org/10.1016/j.scitotenv.2020.141657.

Coulibaly, L.K., Guan, Q., Assoma, T.V., Fan, X., and Coulibaly, N., 2021. Coupling linear spectral unmixing and RUSLE2 to model soil erosion in the Boubo coastal watershed, Côte d'Ivoire. Ecological Indicators, 130. https://doi.org/10.1016/j.ecolind.2021.108092.

Cristiano, E., ten Veldhuis, M.C., and van de Giesen, N., 2017. Spatial and temporal variability of rainfall and their effects on hydrological response in urban areas – a review. Hydrology and Earth System Sciences, 21 (7), Pp. 3859-3878. https://www.doi.org/10.5194/hess-21-3859-2017.

David, E., Fantina, P., 2012. A Comparison of Runoff Estimation Techniques.

Devia, G.K., Ganasri, B.P., and Dwarakish, G.S., 2015. A Review on Hydrological Models. Aquatic Procedia, 4, Pp. 1001-1007. https://www.doi.org/10.1016/j.aqpro.2015.02.126.

Elhakeem, M., and Papanicolaou, A.N., 2009. Estimation of the Runoff Curve Number via Direct Rainfall Simulator Measurements in the State of Iowa, USA. Water Resources Management, 23 (12), Pp. 2455-2473. https://www.doi.org/10.1007/s11269-008-9390-1.

Faizalhakim, A., Nurhidayu, S., Norizah, K., 2018. SCS-Curve Number in Tropics: Is It Reliable?

Fan, F., Deng, Y., Hu, X., and Weng, Q., 2013. Estimating Composite Curve Number Using an Improved SCS-CN Method with Remotely Sensed Variables in Guangzhou, China. Remote Sensing, 5 (3), Pp. 1425-1438. https://doi.org/10.3390/rs5031425.

Foster, G.R., and Meyer, L.D., 1972. Transport of Soil Particles by Shallow Flow. Transactions of the ASAE, 15 (1), Pp. 0099–0102. https://www.doi.org/10.13031/2013.37840

Fu, S., Sonnenborg, T.O., Jensen, K.H. and He, X., 2011. Impact of Precipitation Spatial Resolution on the Hydrological Response of an Integrated Distributed Water Resources Model. Vadose Zone Journal, 10 (1), Pp. 25-36. https://www.doi.org/10.2136/vzj2009.0186.

Gajbhiye, S., 2015. Estimation of Surface Runoff Using Remote Sensing and Geographical Information System. International Journal of u- and e-Service, Science and Technology, 8 (4), Pp. 113-122. https://www.doi.org/10.14257/ijunesst.2015.8.4.12.

Gandini, M., and Usunoff, E.J., 2004. Scs curve number estimation using remote sensing ndvi in a gis environment. Journal of Environmental Hydrology, 4.

Gao, G.Y., Fu, B.J., Lü, Y.H., Liu, Y., Wang, S., and Zhou, J., 2012. Coupling the modified SCS-CN and RUSLE models to simulate hydrological effects of restoring vegetation in the Loess Plateau of China. Hydrology and Earth System Sciences, 16 (7), Pp. 2347-2364. https://www.doi.org/10.5194/hess-16-2347-2012.

Garcia, R., Santiago, B., Noemí, L.R., Estela, N.R. and Artemi, C., 2016. Ongoing and Emerging Questions in Water Erosion Studies. Land Degradation & Development, 28 (1), Pp. 5-21. https://www.doi.org/10.1002/ldr.2641.

Gayathri, C., and S.J., 2018. Estimation of Surface Runoff Using Remote Sensing and GIS Techniques for Cheyyar Sub Basin. In: I.J.o.E.R.T. (IJERT) (Editor), ICONNECT - 2k18 Conference Proceedings.

Gebresellassie, Z.D., 2017. Spatial mapping and testing the applicability of the curve number method for ungauged catchments in Northern Ethiopia. International Soil and Water Conservation Research, 5 (4), Pp. 293-301. https://www.doi.org/10.1016/j.iswcr.2017.06.003.

Gonzalez, A., Temimi, M., and Khanbilvardi, R., 2015. Adjustment to the curve number (NRCS-CN) to account for the vegetation effect on hydrological processes. Hydrological Sciences Journal, 60 (4), Pp. 591-605. https://www.doi.org/10.1080/02626667.2014.898119.

Grimaldi, S., Petroselli, A., and Romano, N., 2013. Green-Ampt Curve-Number mixed procedure as an empirical tool for rainfall-runoff modelling in small and ungauged basins. Hydrological Processes, 27 (8), Pp. 1253-1264. https://www.doi.org/10.1002/hyp.9303.

Haan, C.T., Barfield, B.J., and Hayes, J.C., 1994. Design hydrology and sedimentology for small catchments, Academic Press, New York, NY, Pp. 588.

Hairsine, P.B., and Rose, C.W., 1992. Modeling water erosion due to overland flow using physical principles: 1. Sheet flow. Water Resour. Res., 28, Pp. 237–243. https://doi.org/10.1029/91WR02380.

Hajigholizadeh, M., Melesse, A.M., and Fuentes, H.R., 2018. Erosion and Sediment Transport Modelling in Shallow Waters: A Review on Approaches, Models and Applications. Int J Environ Res Public Health, 15 (3). https://www.doi.org/10.3390/ijerph15030518.

Her, Y., 2011. HYSTAR: Hydrology and Sediment Transport Simulation using Time-Area Method, Virginia Polytechnic Institute and State University.

Hong, Y. and Adler, R.F., 2008. Estimation of global SCS curve numbers using satellite remote sensing and geospatial data. International Journal of Remote Sensing, 29 (2), Pp. 471-477. https://doi.org/10.1080/01431160701264292.

Huang, M., Gallichand, J., Wang, Z., and Goulet, M., 2006. A modification to the Soil Conservation Service curve number method for steep slopes in the Loess Plateau of China. Hydrological Processes, 20 (3), Pp. 579-589. https://www.doi.org/10.1002/hyp.5925.

Ibrahim, S., Brasi, B., Yu, Q., and Siddig, M., 2022. Curve number estimation using rainfall and runoff data from five catchments in Sudan. Open Geosciences, 14 (1), Pp. 294-303. https://www.doi.org/10.1515/geo-2022-0356.

Jaafar, H.H., Ahmad, F.A., and El Beyrouthy, N., 2019. GCN250, new global gridded curve numbers for hydrologic modeling and design. Sci Data, 6 (1), Pp. 145. https://www.doi.org/10.1038/s41597-019-0155-x.

Jain, M.K., and Das, D., 2009. Estimation of Sediment Yield and Areas of Soil Erosion and Deposition for Watershed Prioritization using GIS and Remote Sensing. Water Resources Management, 24 (10), Pp. 2091-2112. https://www.doi.org/10.1007/s11269-009-9540-0.

Jain, M.K., Mishra, S.K., and Shah, R.B., 2009. Identification of sediment source and sink areas in a Himalayan watershed using GIS and remote sensing. Land Degradation & Development, 20 (6), Pp. 623-639. https://www.doi.org/10.1002/ldr.952.

Kalin, 2003. Evaluation of Sediment Transport Models and Comparative Application of Two Watershed Models.

Karamage, F., Liu, Y., Fan, X., Francis Justine, M., Wu, G., Liu, Y., Zhou, H. and Wang, R., 2018. Spatial Relationship between Precipitation and Runoff in Africa. Hydrol. Earth Syst. Sci. . https://www.doi.org/10.5194/hess-2018-424.

Khaddor, I., Achab, M., and Alaoui, A.H., 2015. Simulation of Rainfall-Runoff using GIS, Hydrologic Modeling System and SCS Curves Number: Application to the Meghougha Watershed (Tangier, NW Morocco). European Journal of Scientific Research, 130 (1), Pp. 31 - 45.

Kim, N., and Shin, M.J., 2018. Estimation of Peak Flow in Ungauged Catchments Using the Relationship between Runoff Coefficient and Curve Number. Water, 10 (11). https://www.doi.org/10.3390/w10111669.

Kim, N.W., and Lee, J., 2008. Temporally weighted average curve number method for daily runoff simulation. Hydrological Processes, 22 (25), Pp. 4936-4948. https://www.doi.org/10.1002/hyp.7116.

Kim, N.W., and Shin, M.J., 2019. Curve Number Estimation of Ungauged Catchments considering Characteristics of Rainfall and Catchment. KSCE Journal of Civil Engineering, 23 (4), Pp. 1881-1890. https://www.doi.org/10.1007/s12205-019-0532-1.

Kinnell, 2010. Event soil loss, runoff and the Universal Soil Loss Equation family of models: A review. Journal of Hydrology, 385 (1-4), Pp. 384-397. https://www.doi.org/10.1016/j.jhydrol.2010.01.024.

Komuscu, A.U., and Legate, D.R., 1999. Effects of rainfall variability on spatial accumulation of peak runoff and excess runoff depth: little washita river basin, Oklahoma, USA. Journal of Environmental Hydrology, 7 (18), Pp. 1-25.

Köylü, Ü., and Geymen, A., 2016. GIS and remote sensing techniques for the assessment of the impact of land use change on runoff. Arabian Journal of Geosciences, 9 (7). https://doi.org/10.1007/s12517-016-2514-7.

Laflen, J.M., Lane, L.J., and Foster., G.R., 1991. WEPP: A new generation of erosion prediction technology. Journal of Soil and Water Conservation, 46 (1), Pp. 34-38.

Lal, R., 2009. Soil erosion and sediment transport research in tropical Africa. Hydrological Sciences Journal, 30 (2), Pp. 239-256. https://www.doi.org/10.1080/02626668509490987.

Lanckriet, S., Asfaha, T., Frankl, A., Zenebe, A., and Nyssen, J., 2016. Sediment in Alluvial and Lacustrine Debris Fans as an Indicator for Land Degradation Around Lake Ashenge (Ethiopia). Land Degradation & Development, 27 (2), Pp. 258-269. https://www.doi.org/10.1002/ldr.2424.

Li, X., Qiu, J., Shang, Q., and Li, F., 2016. Simulation of Reservoir Sediment Flushing of the Three Gorges Reservoir Using an Artificial Neural Network. Applied Sciences, 6 (5). https://www.doi.org/10.3390/app6050148.

Liangyun, L., Xiao, Z., Xidong, C., Yuan, G., and Jun, M., 2020. GLC_FCS30: Global land-cover product with fine classification system at 30 m using time-series Landsat imagery (Version v1). [Data set], Zenodo. http://doi.org/10.5281/zenodo.3986872.

Matomela, N., Tianxin, L., Morahanye, L., Bishoge, O.K., and Ikhumhen, H.O., 2019. Rainfall-runoff estimation of Bojiang lake watershed using SCS-CN model coupled with GIS for watershed management. Journal of Applied and Advanced Research, Pp. 16-24. 10.21839/jaar.2019.v4i1.263.

Meshram, S.G., Sharma, S.K., and Tignath, S., 2015. Application of remote sensing and geographical information system for generation of runoff curve number. Applied Water Science, 7 (4), Pp. 1773-1779. 10.1007/s13201-015-0350-7.

Mishra S.K., and V.P., S., 2003. Soil Conservation Service Curve Number (SCS-CN) Methodology, 42. kluwer Academic Publishers, Baton Rouge, U.S.A. https://www.doi.org/10.1007/978-94-017-0147-1.

Nagarajan, N., and Poongothai, S., 2012. Spatial Mapping of Runoff from a Watershed Using SCS-CN Method with Remote Sensing and GIS. Journal of Hydrologic Engineering, 17 (11), Pp. 1268-1277. https://doi.org/10.1061/(asce)he.1943-5584.0000520.

Neitsch, S.L., Arnold, J.G., Kiniry, J.R., and Williams, J.R., 2011. Soil and Water Assessment Tool Theoretical Documentation Version 2009.

NRCS, 1986. Urban Hydrology for Small Watersheds (TR-55). Washington.

NRCS, U., 2009. Hydrologic Soil Groups.

Patel, J.N., and Thorvat, A.R., 2016. Synthetic Unit Hydrograph Development for Ungauged Basins Using Dimensional Analysis. Journal - American Water Works Association, 108, Pp. E145-E153. https://www.doi.org/10.5942/jawwa.2016.108.0014.

Ponce, V.M., and Hawkins, R.H., 1996. Runoff Curve Number: Has It Reached Maturity? Journal of Hydrologic Engineering. Journal of Hydrologic Engineering, 1 (1), Pp. 11–19. https://www.doi.org/10.1061/(asce)1084-0699(1996)1:1(11)

Rawat, K.S., and Singh, S.K., 2017. Estimation of Surface Runoff from Semi-arid Ungauged Agricultural Watershed Using SCS-CN Method and Earth Observation Data Sets. Water Conservation Science and Engineering, 1 (4), Pp. 233-247. https://doi.org/10.1007/s41101-017-0016-4.

Reisenbüchler, M., Bui, M.D., and Rutschmann, P., 2021. Reservoir Sediment Management Using Artificial Neural Networks: A Case Study of the Lower Section of the Alpine Saalach River. Water, 13 (6). https://www.doi.org/10.3390/w13060818.

Rietz, D., and Hawkins, R.H., 2001. Effects of Land Use on Runoff Curve Number. Watershed Management and Operations Management. https://www.doi.org/10.1061/40499(2000)110

Roo, A.P.J.D., 1998. Modelling runoff and sediment transport in catchments using GIS. Hydrological Processes, 12, Pp. 905-922.

Roose, 1996. Land husbandry: Components and strategy.

Ross, C.W., Prihodko, L., Anchang, J., Kumar, S., Ji, W., and Hanan, N.P., 2018. HYSOGs250m, global gridded hydrologic soil groups for curve-number-based runoff modeling. Sci Data, 5: 180091. https://www.doi.org/10.1038/sdata.2018.91.

Rossman, L.A., 2010. Storm Water Management Model User's Manual Version 5.0.

Sachan, S., Kumar, A. and Singh, P.V., 2015. Hyetograph -hydrograph transformation model for uniform and non-uniform rainfall distribution patterns. Journal of Soil and Water Conservation, 4 (3), Pp. 213-218.

Sébastien, O.K., Denis, Y.K., Salla, M., and Félix, T.Z., 2013. Water Quality Assessment of the Coastal Tropical River'Sboubo (Côte d'Ivoire): Physico-Chemical and Biological Aspects. Journal of Environment Pollution and Human Health, 1 (2), Pp. 9-15. https://www.doi.org/10.12691/jephh-1-2-1.

Servat, E., and Dezetter, A., 1993. Rainfall-runoff modelling and water resources assessment in northwestern Ivory Coast. Tentative extension to ungauged catchments. Journal of Hydrology, 148 (1-4), Pp. 231–248. https://www.doi.org/10.1016/0022-1694(93)90262-8

Seydou, D., Dabissi, N., Armand, T.B.Z., Amidou, D., Bamory, K., Rose, E.K., Lanciné, G.D., Serge, K.E., Thierry, K.J., Paturel, J.E., Perrin, J.-L. and Seguis, L., 2018. Effets De La Dynamique Du Couvert Végétal Sur Les Écoulements Dans Le Bassin Versant De La Lagune Aghien En Côte d'Ivoire. European Scientific Journal ESJ, 14 (36). https://www.doi.org/10.19044/esj.2018.v14n36p312.

Sharafati, A., Haji Seyed Asadollah, S.B., Motta, D., and Yaseen, Z.M., 2020. Application of newly developed ensemble machine learning models for daily suspended sediment load prediction and related uncertainty analysis. Hydrological Sciences Journal, 65 (12), Pp. 2022-2042. https://www.doi.org/10.1080/02626667.2020.1786571.

Sitterson, J., Knightes, C., Parmar, R., Wolfe, K., Muche, M. and Avant, B., 2017. An Overview of Rainfall-Runoff Model Types.

Srinivas, G.S., Moorthy, D.V.S., Kumar, Y.Y., and P.J., 2020. Surface Runoff Estimation using RS and GIS - A Case Study of Swarnamukhi River, India. International Journal of Science and Research (IJSR), 9 (5), Pp. 780-784. https://www.doi.org/10.21275/sr20512084915.

Srinivasulu, S., and Jain, A., 2009. Rainfall-Runoff Modelling: Integrating Available Data and Modern Techniques. In: S.L.M. Abrahart R.J., Solomatine D.P. (Editor), Practical Hydroinformatics. Water Science and Technology Library, Springer, Berlin, Heidelberg, pp. 59–70. https://www.doi.org/10.1007/978-3-540-79881-1_5

Strapazan, C., and PetruȚ, M., 2017. Application of ARC HYDRO and HEC-HMS model techniques for runoff simulation in the headwater areas of Covasna watershed (Romania). Geographia Technica, 12 (1), Pp. 95-107. https://www.doi.org/10.21163/gt_2017.121.10.

USDA, N., 2004a. Estimation of Direct Runoff from Storm Rainfall.

USDA, N., 2004b. Hydrologic Soil-Cover Complexes.

USDA-ARS, 2013. Science Documentation. Revised Universal Soil Loss Equation Version 2 (RUSLE2): (for the model with release date of May 20, 2008), Agricultural Research Service. https://www.ars.usda.gov/ARSUserFiles/60600505/RUSLE/RUSLE2_Science_Doc.pdf (accessed 12 April 2021).

Van Dijk, A.I.J.M., Brakenridge, G.R., Kettner, A.J., Beck, H.E., De Groeve, T., and Schellekens, J., 2016. River gauging at global scale using optical and passive microwave remote sensing. Water Resources Research, 52 (8), Pp. 6404-6418. https://www.doi.org/10.1002/2015wr018545.

Van Rompaey, A.J.J., Verstraeten, G., Van Oost, K., Govers, G., and Poesen, J., 2001. Modelling mean annual sediment yield using a distributed approach. Earth Surface Processes and Landforms, 26 (11), Pp. 1221-1236. https://doi.org/10.1002/esp.275.

Vanmaercke, M., Poesen, J., Broeckx, J., and Nyssen, J., 2014. Sediment yield in Africa. Earth-Science Reviews, 136, Pp. 350-368. https://www.doi.org/10.1016/j.earscirev.2014.06.004.

Verma, S., Verma, R.K., Mishra, S.K., Singh, A. and Jayaraj, G.K., 2017. A revisit of NRCS-CN inspired models coupled with RS and GIS for runoff estimation. Hydrological Sciences Journal, 62 (12), Pp. 1891-1930. https://www.doi.org/10.1080/02626667.2017.1334166.

Victor, M., 2017. Chapter 9: Hydrologic Soil-Cover Complexes.

Vojtek, M., and Vojteková, J., 2016. GIS-based Approach to Estimate Surface Runoff in Small Catchments: A Case Study. Quaestiones Geographicae, 35 (3), Pp. 97–116. https://www.doi.org/10.1515/quageo-2016-0030.

Walling, D.E., 2009. the Impact of Global Change on Erosion and Sediment Transport by Rivers: Current Progress and Future Challenges.

Wang, S., Flanagan, D.C., and Engel, B.A., 2019. Estimating sediment transport capacity for overland flow. Journal of Hydrology, 578. https://www.doi.org/10.1016/j.jhydrol.2019.123985.

Wang, Z., Yang, X., Liu, J. and Yuan, Y., 2015. Sediment transport capacity and its response to hydraulic parameters in experimental rill flow on steep slope. Journal of Soil and Water Conservation, 70 (1), Pp. 36-44. https://doi.org/10.2489/jswc.70.1.36.

Xiao, H., Liu, G., Liu, P., Zheng, F., Zhang, J., and Hu, F., 2017. Sediment transport capacity of concentrated flows on steep loessial slope with erodible beds. Sci Rep, 7 (1), Pp. 2350. https://www.doi.org/10.1038/s41598-017-02565-8.

Young, C.B., McEnroe, B.M., and Rome, A.C., 2009. Empirical Determination of Rational Method Runoff Coefficients. Journal of Hydrologic Engineering, 14 (12), Pp. 1283–1289. https://www.doi.org/10.1061/共ASCE禿HE.1943-5584.0000114.

Zhan, X., and Huang, M.L., 2004. ArcCN-Runoff: an ArcGIS tool for generating curve number and runoff maps. Environmental Modelling & Software, 19 (10), Pp. 875-879. https://doi.org/10.1016/j.envsoft.2004.03.001.

Zhang, G.H., Liu, Y.M., Han, Y.F., and Zhang, X.C., 2009. Sediment Transport and Soil Detachment on Steep Slopes: II. Sediment Feedback Relationship. Soil Science Society of America Journal, 73 (4), Pp. 1298-1304. https://www.doi.org/10.2136/sssaj2009.0074.

Zhu, X., Liu, W., Jiang, X.J., Wang, P., and Li, W., 2018. Effects of land-use changes on runoff and sediment yield: Implications for soil conservation and forest management in Xishuangbanna, Southwest China. Land Degradation & Development, 29 (9), Pp. 2962-2974. https://www.doi.org/10.1002/ldr.3068.